ELSEVIER

www.elsevier.nl/locate/jorganchem

Journal of Organometallic Chemistry 613 (2000) 77–85

Journal of Organo metallic Chemistry

Rhodium and palladium complexes from 1,1′ and 1,2 ferrocenylphosphine as bidentate ligands. Versatile coordination

Roland Broussier [a,*], Emmanuelle Bentabet [a], Myriam Laly [a], Philippe Richard [a], Lyudmila G. Kuz'mina [c], Philippe Serp [b], Nigel Wheatley [b], Philippe Kalck [b], Bernard Gautheron [a]

[a] *Laboratoire de Synthèse et d'Electrosynthèse Organométalliques (UMR 5632), Université de Bourgogne, 6, boulevard Gabriel, 21000 Dijon, France*

[b] *Laboratoire de Catalyse et Chimie fine, Ecole Nationale Supérieure de Chimie de Toulouse,118, route de Narbonne, 31077 Toulouse cedex, France*

[c] *N.S. Kursakov Institute of General Inorganic Chemistry, RAS, Leninskiiprosp. 31, 117907 Moscow, Russia*

Received 16 June 2000; accepted 11 July 2000

Abstract

The complexation of the mixed bidentate ligands 1-diphenylphosphino-1′-diphenylthiophosphinoferrocenyl and 1,2-bis-(diphenylphosphino)ferrocenyl with rhodium(I) and palladium(II) species yield a range of mono- and dirhodium or palladium complexes. Their interest as possible catalysts for alkene hydroformylation and alkoxycarbonylation and Heck coupling reactions has been assessed. $Fe[C_5Me_4P(S)Ph_2][C_5Me_4PPh_2]PdCl_2$ and $Fe[C_5H_2\text{-}1,2\text{-}(PPh_2)_2\text{-}4\text{-}{}^tBu][C_5H_5]PdCl_2$ have been characterized by single-crystal X-ray diffraction studies. © 2000 Elsevier Science B.V. All rights reserved.

Keywords: Ferrocene; Phosphine; Rhodium; Palladium; Catalysis

---

1. Introduction

The on-going interest in ferrocene chemistry stems from an important advantage of the ferrocenyl architecture: for chelating substituents, their coordination ability may be fine tuned by the choice of the number and the relative positioning of these substituents and by the possible presence of other groups.

In the context of our research into rhodium and palladium compounds of catalytic utility, we were interested in the effect of chelation on the stoechiometry and coordination modes in complexes of ferrocenylphosphines with rhodium(I) and palladium(II).

We have indeed observed differences in the behavior of the two platinum group metal with rhodium being more sensitive than palladium to the influence of the ligands.

We report here the reactions of $[RhCl(CO)_2]_2$ with the metalloligands **1** and **2** (Scheme 1) and of $[Rh(S^tBu)(CO)_2]_2$ with **2**, which supplements the study already published [1] with **3**. These ligands give a range of di- and polynuclear complexes with Rh(I), whereas the reaction with $PdCl_2$ led in each case to dinuclear derivatives.

These compounds have been screened as possible homogeneous catalysts for carbonylation and C–C coupling reactions.

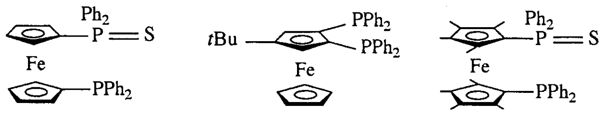

1 **2** **3**

Scheme 1.

---

* Corresponding author. Tel.: +33-380-396100/03; fax: +33-380-396100.

E-mail address: roland.broussier@u-bourgogne.fr (R. Broussier).

0022-328X/00/$ - see front matter
PII: S0022-328X(00)00501-5

2. Results and discussion

2.1. Rhodium complexes

2.1.1. Preparation of the complexes

The complexes obtained from the reaction of ligands **1** and **2** with $[\mathrm{RhCl(CO)_2}]_2$ and of ligand **2** with $[\mathrm{Rh(S^tBu)(CO)_2}]_2$ are shown in Scheme 2.

The reaction of the phosphine–thiophosphine ligand **1** with 0.5 equivalent $[\mathrm{RhCl(CO)_2}]_2$ (equimolar quantities of Fe and Rh) in toluene gave two products: the expected dinuclear species **4** and a trinuclear species **5** in which rhodium(I) centers are linked by a single μ-chloro bridge. Compound **5** is neutral, as opposed to the cationic tetranuclear species formed in the analogous reaction with the ring-permethylated analogue of **1** [1]. In the present case, the less sterically hindered ligand shows fewer propensities to substitute the carbonyl ligands, indicating the importance of the electronic effects of ring substitution in these systems. When the reaction is carried out in dichloromethane, only the 1:1 complex **4** is produced. In order to obtain **5** in a pure form, it was necessary to use an excess of $[\mathrm{RhCl(CO)_2}]_2$.

The reaction of **2** with $[\mathrm{RhCl(CO)_2}]_2$ gave a more complex reaction mixture and three products **6**, **8a** and **8b** were characterized. The formation of a cationic rhodium complex **8** stabilized by four phosphorus atoms has also been observed with dppf [2], but here the disymmetrical substitution of the ferrocene leads to *cis–trans* isomerism. The ^{31}P-NMR spectrum indicates an isomer ratio of 7:3, but we have been unable to separate them, and consequently we did not try to assign the signals to one or the other. Working under a carbon monoxide atmosphere allows **6** to be cleanly synthesized separately from **8a** and **8b**. The isomer mixture **8a** and **8b**, obtained together with **6** in toluene, is easily isolated as a precipitate associated with the counterion $[\mathrm{RhCl_2(CO)_2}]^-$ (ν_{CO}: 1990, 2068 cm^{-1}). The two isomers **9a** and **9b**, with Cl^- as counterion, can also be obtained from **6**, by the addition of an excess of ligand.

It is known that $[\mathrm{Rh(S^tBu)(CO)_2}]_2$ retains its dinuclear framework on reaction with diphosphines [3,4]: the diphosphine acts as a supplementary bridging ligand between the two rhodium atoms. In contrast, on reaction of the ligand **2** with $[\mathrm{Rh(S^tBu)(CO)_2}]_2$, we obtained a novel species **7**, in which the diphosphine is bounded to only one rhodium atom. This can be attributed to the rigidity of the ligand with a short distance between the phosphorus atoms and the global planar geometry of the substituted cyclopentadienyl ring.

With regard to the use of the spectroscopic methods to establish the molecular structures, the form of the ^{31}P-NMR spectrum for **6** and **7** and the presence of several absorption bands in the infrared spectrum of **5** should be mentioned. For **6** and **7** the two phosphorus atoms are nonequivalent and the ^{31}P signal (dd) results from mutual coupling ($^2J_{\mathrm{P-P}}$) and vicinal coupling ($J_{\mathrm{P-Rh}}$) with the rhodium atom. The IR absorptions in the CO region for compound **5** (1992, 2003 and 2078 cm^{-1}) are very similar to those of $\mathrm{(CO)_2ClRh(\mu\text{-}Cl)Rh(CO)\{C_6H_5P[OC(CH_3)_2CH_2]_2NH\}}$ [5] (1998, 2008 and 2074 cm^{-1}), which exhibits the same geometry and coordination as **5** Table 1.

Table 1
NMR and IR data for **4**, **5**, **6**, **7**, **8a** and **8b**.

Compound	NMR ^{31}P δ, ppm (J, Hz)	IR νCO, cm^{-1}
4	19.1 (142) and 39.7	1971
5	36.6 (136) and 44.8	1992, 2003, 2078
6	31.0 dd (108/36) and 54.0 dd (127/36)	2011
7	31.0 dd (130/40) and 44.0 dd (126/40)	1977
8a,b	37.0 or 39.0 (135)	

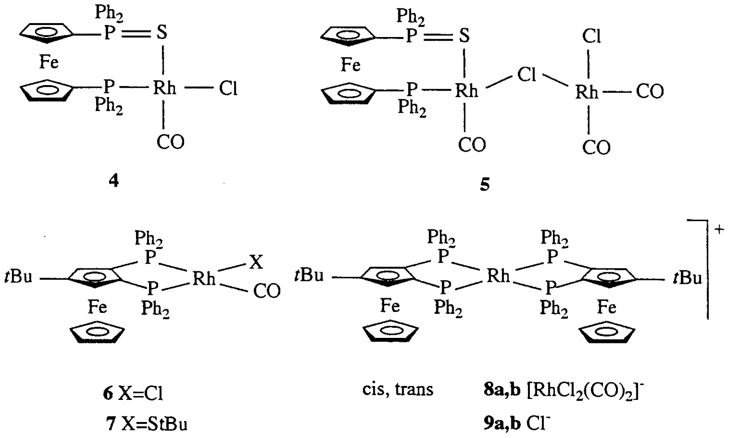

Scheme 2.

Table 2
Hydroformylation of oct-1-ene by complexes **4**, **13**, **6** and **7** [a]

Precursor	t (h)	Pressure (bar)	$P(OPh)_3/Rh$	Yield in aldehyde (%)	Selectivities			
					Nonanal	2-Methyl octanal	2-Ethyl heptanal	2-Propyl hexanal
4 [b]	16	10	0	0				
4 [b]	16	10	6	0				
13 [b]	16	10	0	0				
13 [b]	16	10	6	61	84.5	15.5		
6 [c]	16	10	0	34	69	30.5	0.5	
6 [b]	16	50	0	96	45.7	35.5	10.6	8.2
6 [b]	4	50	0	86.9	49.5	35.7	9.1	5.7
7 [c]	16	10	0	94	52	48		

[a] Temperature: 80°C.
[b] Alkene/catalyst = 200.
[c] Alkene/catalyst = 215.

2.1.2. Catalytic hydroformylation

Table 2 shows the results of the hydroformylation of oct-1-ene catalyzed by compounds **4**, **6**, **7** and **13** ($Fe[C_5Me_4P(S)Ph_2][C_5Me_4PPh_2]RhCl(CO)$ [1]). At 10 bar, the presence of a sulfur atom on one phosphorus atom seems to inhibit the reaction. However, the addition of six molar equivalents of $P(OPh)_3$ to complex **13**, but not to complex **4**, leads to a 61% yield of aldehydes. The difference of reactivity may come from the lower basicity of the metal center for **13** ($\nu CO = 1987$ cm^{-1}) than for **4** (1971 cm^{-1}), resulting from the electronic influence of the methyl substituents on the cyclopentadiene rings. An intermediate species of general formula RhH(CO)(P,PS) is expected.

When using ligand **2** (complexes **6** and **7**), a different reactivity is observed. Reaction occurs without the addition of auxiliary $P(OPh)_3$, with a yield in aldehydes of 34 and 94% for **6** and **7**, respectively. At the end of these experiments, catalytic solutions were clear (no rhodium precipitation) and the complexes were recovered without transformation. The differences in reactivity between **6** and **7** could stem from the ease of production of an active hydride species. This step should be enhanced on **7**, which presents a more basic metal center. The unexpected formation of small amounts of 2-ethylheptanal using precursor **6** prompted us to repeat the experiment at a higher pressure (50 bar): under these conditions, all the isomeric aldehydes (nonanal/2-methyloctanal/2-ethylheptanal/2-propylhexanal) were detected, in a ratio of: 46/36/10/8. This unusual activity for the hydroformylation of internal olefins was confirmed by the use of cyclohexene as substrate: under the same conditions a 44% yield of cyclohexanecarboxaldehyde was obtained.

As part of an on-going interest in the catalytic transformation of natural products, we also examined the activity of **6** and **7** for the hydroformylation of two monoterpenes, namely α- and β-pinene. Neither complex could activate the internal double bond of α-pinene under the relatively mild conditions employed (20 bar, 85°C, 18 h). However, both showed a certain activity for the hydroformylation of β-pinene, with 10-formylpinane yields of 2.5% (**6**) and 11% (**7**) and diastereoisomeric excesses of 56% (**6**) and 48% (**7**) for the *cis* diastereoisomer. Isomerization was a competing reaction (5% yield of α-pinene) in the case of **7**.

2.2. Palladium coordination

2.2.1. Preparation of the complexes

The monomeric palladium complexes L_2PdCl_2 **10**, **11** and **12** have been obtained (Scheme 3) by reaction of **1**, **2** and **3**, respectively with either $PdCl_2$ and $(PhCN)_2PdCl_2$. The route appears to be specific and the formation of mixtures of products is not observed unlike in the case of rhodium. Complexation produces a large downfield shift of the ^{31}P(III)-NMR resonance compared to that of the starting ligand (**1** $\delta -19.6$, s and **10** $\delta +12.6$, s; **2** $\delta -24.3$, s and **11** $\delta +42.0$ s; **3** $\delta -24.9$ s and **12** $\delta +28.0$ s).

2.2.2. X-ray structures of 11 and 12

Single-crystals of **11** and **12** which were suitable for diffraction analysis were obtained by recrystallization in CH_2Cl_2.

The solid-state structures of the compounds are shown in Figs. 1 and 2, respectively.

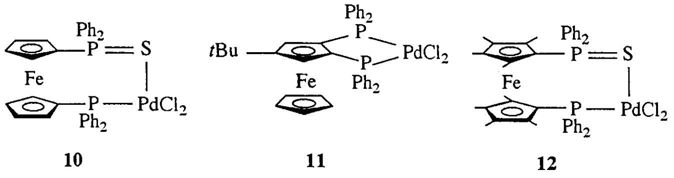

Scheme 3.

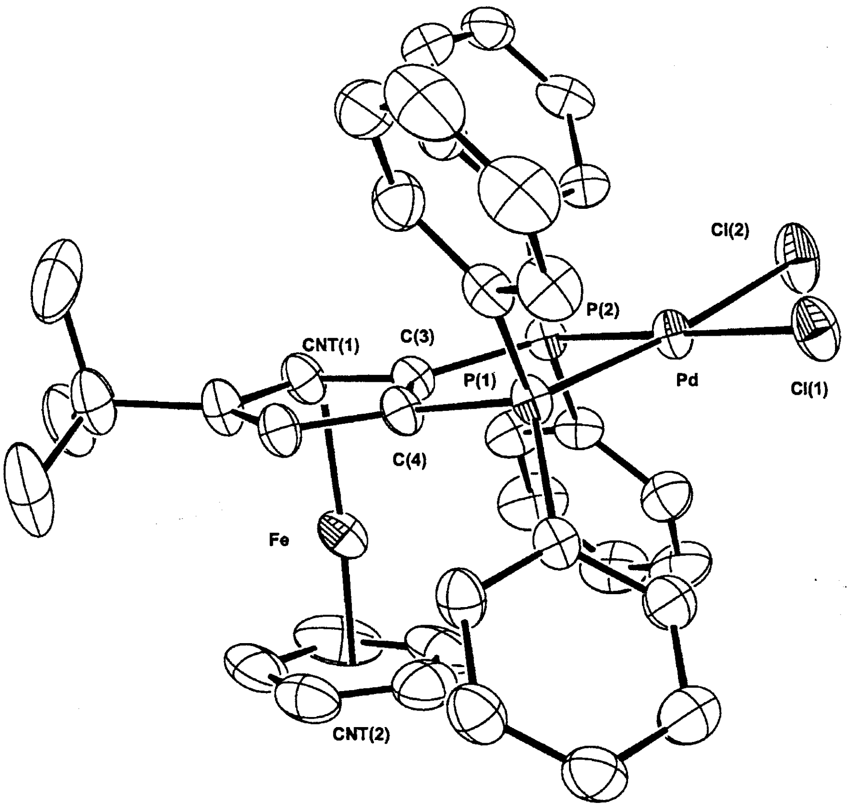

Fig. 1. ORTEP view [16] of **11** drawn at the 30% probability level. Hydrogen atoms and the CH_2Cl_2 solvate molecule are omitted for clarity.

Pertinent bond distances and angles are listed in Table 3. The parameters describing the geometrical environment of the palladium atom are compared in Table 4 with those of complexes of similar chelating ligands: dppf [6,7] and (R)(S)BPPFA [8]. Data collection and refinement parameters are given in Table 5.

For **11** the square planar coordination of the Pd atom is very slightly distorted. The chelated P–Pd–P angle of 88.97(4)° leads to an opening of the Cl–Pd–Cl angle to 92.53(5)°. The phosphorus atoms are displaced from the plane of the Cp ring by 0.25 Å for P(1) and 0.17 Å for P(2) (*exo*-type) and the coordination plane of the palladium is tilted from the plane of the Cp ring by 11.8(2)°. The ferrocenyl part shows a usual tilt of Cp planes (3.1°) and an eclipsed conformation (twist angle 3.0°), whereas it is clearly staggered for the free ligand **2** (twist angle: 27.0° [11]). As one would expect, the Fe-centroid (CNT) distance is shorter for the substituted ring (1.652 Å) than for the non-substituted (1.673 Å) [11].

The square planar geometry in molecule **12** is significantly distorted by the difference in the *trans* influences of the phosphorous center and the phosphine sulfide center, with the Pd–Cl bond *trans* to phosphorous being 0.05 Å longer than that *trans* to sulfur. The length and the zigzag geometry of the [4]-ferrocenophane bridge involves the shortest bite angle com-

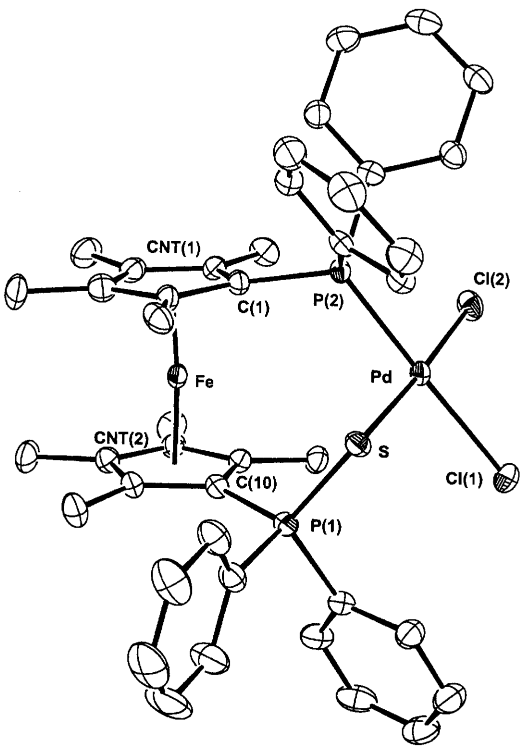

Fig. 2. ORTEP view [16] of **12** drawn at the 30% probability level. Hydrogen atoms and the CH_2Cl_2 solvate molecule are omitted for clarity.

Table 3
Bond lengths (Å) and angles (°) for **11** and **12**.

11		12	
Fe–CNT(1)	1.652	Fe–CNT(1,5)	1.675
Fe–CNT(2)	1.673	Fe–CNT(6,9)	1.683
Pd–P(1)	2.2457(11)	Pd–S	2.3278(7)
Pd–P(2)	2.2405(12)	Pd–P(2)	2.2445(7)
Pd–Cl(1)	2.3518(13)	Pd–Cl(1)	2.3696(7)
Pd–Cl(2)	2.3440(12)	Pd–Cl(2)	2.3160(7)
P(1)–C(4)	1.800(4)	P(1)–C(10)	1.795(3)
P(2)–C(3)	1.797(4)	P(2)–C(1)	1.815(3)
		P(1)–S	2.0237(9)
CNT(1)–Fe–CNT(2)	176.4	CNT–Fe–CNT	173.5
P(1)–Pd–P(2)	88.97(4)	S–Pd–P(2)	85.75(2)
Cl(1)–Pd–Cl(2)	92.53(5)	Cl(1)–Pd–Cl(2)	89.41(3)
P(1)–Pd–Cl(1)	90.64(5)	S–Pd–Cl(1)	92.80(3)
P(1)–Pd–Cl(2)	174.88(6)	S–Pd–Cl(2)	176.32(2)
P(2)–Pd–Cl(1)	179.41(5)	P(2)–Pd–Cl(1)	176.29(3)
P(2)–Pd–Cl(2)	87.84(5)	P(2)–Pd–Cl(2)	92.22(2)
C(4)–P(1)–Pd	107.1(2)	C(1)–P(2)–Pd	114.40(9)
C(3)–P(2)–Pd	107.0(2)	C(10)–P(1)–S	118.08(9)
		P(1)–S–Pd	107.13(3)

pared to those reported for [3]-ferrocenophanes (Table 4). In the [4]-ferrocenophane **12**, the Cp rings are in a staggered conformation as in the [3]-ferrocenophane (**12**: twist angle 32.4°; P···P distance 4.361 Å and P–Pd–S–P length 6.596 Å compared to dppf, CHCl$_3$ [6]: P···P 3.487 Å and P–Pd–P 4.564 Å). At the same time, the two Cp rings are nearly parallel (tilt angle 4.6°) and the P atoms are displaced from the plane of the corresponding ring, away from the Fe atom by 0.265 Å (P(2)) and 0.175 Å (P(1)).

2.2.3. Catalytic activity in methoxycarbonylation and Heck reactions

Among the numerous palladium-catalyzed C–C bond formation reactions, we investigated two examples with different potential applications: methoxycarbonylation which transforms an alkene into a methyl ester in the presence of carbon monoxide and an alcohol, and the Heck reaction, in which an alkene is substituted.

The methoxycarbonylation of oct-1-ene gave disappointing results. Under the usual experimental conditions (95°C, 40 bar) in the presence of 2.5 equivalents of SnCl$_2$ per palladium [9] only **10** presents any activity (esters 8%: methyl nonanoate 84%, methyl2-methyloctanoate 16%). Further studies are continuing focussing on the nature of hydride complexes formed under these conditions.

Boyes and co-workers [10] reported that certain palladium complexes of ferrocenyl diphosphine ligands, particularly PdCl$_2$(diisoppf) (diisoppf = 1,1′-bis(diisopropylphosphino)ferrocene), were active catalysts for the Heck coupling reaction. We tested compounds **10**–**12** under the same conditions (reaction of phenyl iodide and methyl acrylate to give methyl *trans*-cinnamate), and found very promising activity for **10** (yield 90%) and **12** (yield 99%; c.f. PdCl$_2$(diisoppf), 96%). The poor yield (5%) obtained with **11** is comparable to that observed with PdCl$_2$(dppf) (7%). These results seem to indicate that the reaction is primarily dependent upon the electronic effects given by the ligand and can be viewed as the result of the hemilabilisation of diisoppf as well as that of **10** and **12**.

3. Experimental

3.1. General considerations

All manipulations were performed under Argon using standard Schlenk tube techniques. Mass spectra (electronic ionization 70 eV) were recorded on a Kratos concept IS machine. ^{1}H- and ^{31}P{^{1}H}-NMR spectra were recorded on a Bruker AC 200 spectrometer.

The starting compounds **2** [11] and **3** [1] were prepared according to the literature.

*3.2. Preparation of **1***

A suspension of dppf (6.34 g, 11.4 mmol) in 120 ml toluene was added, at 0°C, to a suspension of sulfur (0.36 g, 11.4 mmol) in 30 ml toluene. The mixture was

Table 4
Comparison between X-ray parameters of **11**, **12**, dppf and (R)(S)BPPFA.

	Ligand bite angle (°)	Cl–Pd–Cl (°)	Pd–P (ou Pd–S)	Pd–Cl (Å)
PdCl$_2$[(R)(S)BPPFA] [a]	98.79(4)	87.83(4)	2.302(1) 2.296(1)	2.351(1) 2.334(1)
PdCl$_2$(dppf),CHCl$_3$ [b]	99.07(5)	87.8(1)	2.283(1) 2.301(1)	2.347(1) 2.348(1)
PdCl$_2$(dppf),CH$_2$Cl$_2$ [b]	97.98(4)	89.96(4)	2.278(1) 2.289(1)	2.340(1) 2.358(1)
11	88.97(4)	92.53(5)	2.2457(11) 2.2405(12)	2.3518(13) 2.3440(12)
12	85.75(2)	89.41(3)	Pd–P 2.2445(7) Pd–S 2.3278(7)	2.3160(7) 2.3696(7)

[a] (R)(S)BPPFA = (*R*)-*N*,*N*-dimethyl-1-[(*S*)-1′,2-bis-(diphenylphosphino)ferrocenyl]ethylamine.

[b] dppf = 1,1′-bis-(diphenylphosphino)ferrocene.

Table 5
Crystal data and structure refinement for **11** and **12**

Compound	**11**	**12**
Formula	$C_{39}H_{38}Cl_4FeP_2Pd$	$C_{43}H_{46}Cl_4FeP_2PdS$
Formula weight	872.68	960.85
Temperature (K)	293(2)	150.0(2)
Crystal system	Orthorhombic	Triclinic
Space group	$P2_12_12_1$	$P\bar{1}$
a (Å)	12.065(2)	11.0490(1)
b (Å)	17.250(2)	11.5799(1)
c (Å)	18.230(2)	18.4383(2)
α (°)	90	97.379(1)
β (°)	90	104.510(1)
γ (°)	90	108.720(1)
V (Å^3)	3794.1(9)	2106.25(3)
Z	4	2
F(000)	1768	980
D_{calc} (g cm^{-3})	1.528	1.515
Diffractometer	Nonius CAD-4	Siemens SMART
Scan type	ω	ω
λ (Å)	0.71073	0.71073
μ (mm^{-1})	1.250	1.181
Crystal size (mm^3)	0.50 × 0.41 × 0.32	0.20 × 0.18 × 0.12
$\sin(\theta)/\lambda_{max}$ (Å^{-1})	0.62	0.65
Index ranges	$-15 \leq h \leq 0$, $-21 \leq k \leq 0$, $0 \leq l \leq 22$	$-12 \leq h \leq 14$, $-15 \leq k \leq 12$, $-23 \leq l \leq 23$
Absorption correction	Psi-scan	Empirical (SHELTXTL-PLUS)
Max transmission	0.993	0.783
Min transmission	0.954	0.628
Reflections collected	4285	15 555
Independent reflections	4284	9570 [$R_{int} = 0.0314$]
Reflections observed[$I > 2\sigma(I)$]	3807	8036
Refinement method	Full-matrix least-squares on F^2	Full-matrix least-squares on F^2
Data/restraints/parameters	4284/0/425	8977/0/654
R for IRCGT	R_1 [a] $= 0.0297$ wR_2 [b] $= 0.0771$	R_1 [a] $= 0.0342$ wR_2 [b] $= 0.0767$
R for IRC	R_1 [a] $= 0.0412$ wR_2 [b] $= 0.0826$	R_1 [a] $= 0.0483$ wR_2 [b] $= 0.0957$
Goodness-of-fit [c]	1.034	1.032
Absolute structure parameters	0.06(3)	
Largest difference peak and hole (e Å^{-3})	0.618 and −0.422	0.636 and −0.608

[a] $R_1 = \Sigma(|F_o| - |F_c|)/\Sigma|F_o|$.

[b] $w = 1/[\sigma^2(F_o^2) + (0.047P)^2 + 1.95P]$ for **11** where $P = (\max(F_o^2,0) + 2*F_c^2)/3$ and $wR_2 = \{\Sigma[w(F_o^2 - F_c^2)^2]/\Sigma[w(F_o^2)^2\}^{1/2}$ where $w = 1/[\sigma^2(F_o^2) + (0.030P)^2 + 3.01P]$ for **12**.

[c] Goodness-of-fit $= \{\Sigma[w(F_o^2 - F_c^2)^2]/(N_o - N_v)\}^{1/2}$.

allowed to warm to room temperature (r.t.) and stirred for 18 h. The mixture was filtered and the filtrate evaporated under reduce pressure. The resulting brown residue was chromatographed on a silica column with 3:1 toluene–hexane as eluent.

Three successive orange fractions were obtained: the first one contained dppf, the second contained the expected product and the last one the dithiophosphino compound.

The solvent was removed from the second fraction and gave **1** as a yellow powder (1 g, 1.71 mmol, yield = 15%), m.p. 183°C. Anal. Calc. for $C_{34}H_{28}FeP_2S$: C, 69.66; H, 4.77; S 5.47. Found: C, 69.78; H, 4.76; S 5.25%. ^{1}H-NMR ($CDCl_3$): δ 4.01 (m, 2H, Cp), 4.35 (m, 2H, Cp), 4.38 (m, 2H, Cp), 4.49 (m, 2H, Cp), 7.39 (m, 10 H, Ph), 7.65 (m, 10 H, Ph). ^{31}P{^{1}H}-NMR ($CDCl_3$): δ −19.4 (s), 39.2 (s). EI-MS (200°C), m/z (%): 586 (100) [M^+], 554 (96) [$M^+ - S$], 509 (20) [$M^+ - Ph$], 337 (85) [$M^+ - C_5H_4PPh_2$].

Complex **1** can be obtained by a procedure analogous to that used to prepare **3** [1], using diphenylphosphinocyclopentadienyllithium and diphenylthiophosphinocyclopentadienyllithium. Yield = 8%.

3.3. Preparation of **4**

A solution of **1** (77 mg, 0.13 mmol) and $[RhCl(CO)_2]_2$ (25 mg, 0.065 mmol) in 10 ml dichloromethane was stirred, at r.t. for 2 h. The solvent was removed under reduced pressure and the resulting oil was washed with 10 ml hexane to give an orange powder. The yield was essentially quantitative. Anal. Calc. for $C_{35}H_{28}ClFeOP_2RhS$: C, 55.86; H, 3.72; S 4.26. Found: C, 56.27; H, 3.97; S 4.09%. ^{1}H-NMR ($CDCl_3$): δ 4.30 (m, 2 H, Cp), 4.40 (m, 2 H, Cp), 4.57 (m, 2 H, Cp), 4.83 (m, 2 H, Cp), 7.16–7.69 (m, 20 H, Ph). ^{31}P{^{1}H}-NMR ($CDCl_3$): δ 19.1 (d, 142 Hz), 39.7 (s). MS (FAB), m/z (%): 716 (95) [$M^+ - HCl$], 688 (100) [$M^+ - HCl - CO$], 656 (50) [$M^+ - HCl - CO - S$]. IR (CH_2Cl_2, cm^{-1}): ν(CO) 1971.

3.4. Preparation of **5**

A mixture of **1** (146 mg, 0.25 mmol) and $[RhCl(CO)_2]_2$ (97 mg, 0.25 mmol) in 10 ml toluene was stirred, at r.t. for 1 h. The solvent was removed under reduced pressure and the resulting oil was washed twice with 10 ml hexane to give an orange powder (200 mg, 0.19 mmol, yield = 76%), m.p. 146°C (dec.). Anal. Calc. for $C_{37}H_{28}Cl_2FeO_3P_2Rh_2S$: C, 46.93; H, 2.96; S, 3.38. Found C, 46.66; H, 2.93; S, 3.64%. ^{1}H-NMR ($CDCl_3$): δ 4.13 (m, 2 H, Cp), 4.47 (m, 2 H, Cp), 4.61 (m, 2 H, Cp), 4.93 (m, 2 H, Cp), 7.25–7.70 (m, 20 H, Ph). ^{31}P{^{1}H}-NMR ($CDCl_3$): δ 36.6 (d, 136 Hz), 44.8 (s). MS (FAB): fragmentation as **4**. IR (CH_2Cl_2 cm^{-1}): ν(CO) 2078, 2003, 1992.

3.5. Preparation of **6**

To **2**(300 mg, 0.49 mmol) in 20 ml toluene under CO were added, at r.t. $[RhCl(CO)_2]_2$ (95.5 mg, 0.24 mmol) in 10 ml toluene. After stirring under CO for 45 min the solvent was removed under reduced pressure to give a yellow solid, identified as **6**. The yield was essentially quantitative, m.p. 206°C (dec.). Anal. Calc. for $C_{39}H_{36}ClFeOP_2Rh$: C, 60.29; H 4.68. Found: C, 60.05; H 4.66%. ^{1}H-NMR ($CDCl_3$): δ 1.27 (s, 9H, ^{t}Bu), 3.37 (s, 5H, Cp), 4.35 (s, 1H, Cp), 4,41 (s, 1H, Cp), 7–8.2 (m, 20H, Ph). ^{31}P{^{1}H}-NMR($CDCl_3$):δ 54 (dd, P–Rh–Cl, $^2J_{(P–P)} = 36$ Hz, $^1J_{(P–Rh)} = 164$ Hz), 31 (dd, P–Rh–CO, $^2J_{(P–P)} = 36$ Hz, $^1J_{(P–Rh)} = 127$ Hz). MS (FAB), *m*/*z* (%): 777 (10) [M^+], 747 (60) [($M^+ - CO$)], 712 (70) [($M^+ - COCl$)]. IR (CH_2Cl_2 cm^{-1}): ν_{CO} 2011.

3.6. Preparation of **7**

To **2** (516 mg, 0.84 mmol) in 15 ml toluene were added, at r.t. $[Rh(\mu S^tBu)(CO)_2]_2$ (209 mg, 0.42 mmol) in 5 ml toluene. The solvent was immediately removed under reduced pressure and the residue washed with 15 ml hexane to give an orange powder (273 mg, 0.33 mmol, yield = 78%), m.p. 206°C. Anal. Calc. for $C_{43}H_{45}FeOP_2RhS$: C, 62.20; H 5.47; S, 3.86. Found: C, 61.78; H, 5.48; S, 3.69%. ^{1}H-NMR ($CDCl_3$): δ 1.25 (s, 9H, ^{t}Bu), 1.46 (s, 9H, S^{t}Bu), 3.31 (s, 5H, Cp), 4.29 (s, 1H, CH), 4.35 (s, 1H, CH), 7–8, 11 (m, 20H, Ph). ^{31}P{^{1}H}-NMR($CDCl_3$): δ 44 (dd, P–Rh–S^{t}Bu, $^2J_{(P–P)} =$ 40 Hz, $^1J_{(P–Rh)} = 126$ Hz), 31 (dd, P–Rh–CO, $^2J_{(P–P)} =$ 40 Hz, $^1J_{(P–Rh)} = 130$ Hz). MS (FAB), *m*/*z* (%): 830 (70) [M^+], 802 (50) [($M^+ - CO$)], 741 (40) [($M^+ - S^tBu$)], 712 (100) [($M^+ - S^tBuCO$)]. IR (CH_2Cl_2 cm^{-1}): ν_{CO} 1977.

3.7. Preparation of **8a** and **8b**

To **2** (180 mg, 0.295 mmol) in 20 ml toluene were added, at r.t. $[RhCl(CO)_2]_2$ (57.8 mg, 0.148 mmol) in 10 ml toluene. The resulting precipitate (the filtrate contained **6**) was immediately isolated to give **8a**, and **8b** as an orange powder (108 mg, 0.088 mmol, yield = 59%). Anal. Calc. for $C_{78}H_{72}Cl_2Fe_2O_2P_4Rh_2$: C, 60.29; H, 4.63. Found: C, 60.36; H, 4.80%. ^{1}H-NMR ($CDCl_3$): δ 1.13 (s, 9H, ^{t}Bu), 3.18 (s, 5H, Cp), 4.11 (s, 2H, Cp), 7.0–7.5 (m, 20H, Ph). ^{31}P{^{1}H}-NMR($CDCl_3$):δ 37.0 (d, $^1J_{(P–Rh)} = 135$ Hz), 39.0 (d, $^1J_{(P–Rh)} = 135$ Hz). MS (FAB), *m*/*z* (%): 1324 [M^+]. IR (CH_2Cl_2 cm^{-1}): ν_{CO} 1990 and 2068.

3.8. Preparation of **9a** and **9b**

To **2** (180 mg, 0.295 mmol) in 20 ml toluene were added, at r.t. $[RhCl(CO)_2]_2$ (30 mg, 0.077 mmol) in 10 ml toluene. After stirring at r.t. for 30 min, the solvent was removed under reduced pressure to give **9a** and **9b** as an orange solid. The yield was essentially quantitative. The same mixture can be obtained by mixing **6** and **2** in toluene. Anal. Calc. for $C_{76}H_{72}ClFe_2P_4Rh$: C, 68.94; H, 5.49. Found: C, 68.80; H, 5.47%.

3.9. Preparation of **10**

A suspension of **1** (116 mg, 0.19 mmol) and $PdCl_2$ (35 mg, 0.19 mmol) in 15 ml toluene was stirred, at r.t. for 72 h. The resulting solution was evaporated to dryness giving **10** as an orange–yellow solid (130 mg, 0.17 mmol, yield = 89%), m.p. 201°C. Anal. Calc. for $C_{34}H_{28}Cl_2FeP_2PdS$: C, 53.48; H, 3.67; S, 4.20. Found: C, 53.6; H, 3.66; S, 4.03%. ^{1}H-NMR ($CDCl_3$): δ 4.36 (m, 2 H, Cp), 4.49 (m, 2 H, Cp), 4.59 (m, 2 H, Cp), 4.98 (m, 2 H, Cp), 7.12–7.68 (m, 20 H, Ph). ^{31}P{^{1}H}-NMR ($CDCl_3$): δ 12.6 (s), 38.9 (s). MS (FAB), *m*/*z* (%): 726 (90) [$M^+ - HCl$], 691 (100) [$M^+ - HCl_2$], 613 (90) [$M^+ - HCl_2 - C_6H_6$].

3.10. Preparation of **11**

A mixture of **2** (341 mg, 0.56 mmol) and $(PhCN)_2PdCl_2$ (214 mg, 0.56 mmol) in 20 ml dichloromethane was stirred at r.t. for 48 h. The resulting solution was evaporated to dryness giving **11** as a yellow–brown solid (411 mg, 0.52 mmol, yield = 93%), m.p. > 260°C. Anal. Calc. for $C_{38}H_{36}FeP_2PdCl_2$: C, 57.93; H, 4.62. Found: C, 57.89; H, 4.60%. ^{1}H-NMR ($CDCl_3$): δ 1.27 (s, 9H, ^{t}Bu), 3.40 (s, 5H, Cp), 4,41 (s, 2H, CH), 7,17–8,17 (m, 20H, Ph). ^{31}P{^{1}H}-NMR($CDCl_3$):δ 42,0 (s). EI–MS (200°C), *m*/*z* (%): 787 (15) [M^+], 751 (100) [($M^+ - Cl$)], 716 (20) [($M^+ - 2Cl$)].

3.11. Preparation of **12**

A suspension of **3** (800 mg, 15 mmol) and $PdCl_2$ (200 mg, 1.15 mmol) in 30 ml toluene was stirred, at r.t. for 1 week. The resulting solution was evaporated to dryness giving **12** as a brown solid (870 mg, 0.99 mmol, yield = 86%), m.p. 190°C (dec.). Anal. Calc. for $C_{42}H_{44}CH_2Cl_2Cl_2FeP_2PdS$: C, 53.76; H, 4.79. Found C, 53.5; H, 4.79%. ^{1}H-NMR ($CDCl_3$): δ 1.76 (s, 12 H, Me), 1.80 (s, 6 H, Me), 1.85 (s, 6 H, Me), 7.20–7.64 (m, 20 H, Ph). ^{31}P{^{1}H}-NMR ($CDCl_3$): δ 28.0 (s), 40.9 (s). MS (FAB), *m*/*z* (%): 838 (100) [$M^+ - HCl$], 803 (80) [$M^+ - HCl_2$].

3.12. Hydroformylation of oct-1-ene and α- or β-pinene

The hydroformylation of these alkenes was performed in a magnetically stirred 100 ml stainless steel autoclave with magnetic stirring, charged at constant pressure with an equimolecular mixture of H_2 and CO from a tank. The autoclave was charged with the complex and evacuated. The liquid mixture contained in a Schlenk tube (toluene, alkene, excess of ligand when necessary) was introduced by aspiration. The pressure was kept at 1 bar with nitrogen while the autoclave was heated to 80°C. The H_2:CO gas mixture was then admitted to the desired pressure. After the desired reaction time (usually 16–18 h), the stirring and the heating were stopped and once the temperature had returned to near 25°C the pressure was slowly released. The reaction mixture was transferred under nitrogen in a Schlenk tube for analyses by GC. For oct-1-ene, anisole was used as internal standard.

3.13. Methoxycarbonylation of oct-1-ene

The procedure was similar to the above, except that a 200 ml autoclave with mechanical stirring was used, at a pressure of 40 bar of CO and a temperature of 95°C. A typical reaction mixture contained 0.15 mmol $PdCl_2L_2$, 0.375 mmol $SnCl_2$, 15 mmol oct-1-ene, 30 mmol methanol, 30 ml toluene, and 1.2 ml dodecane (internal standard).

3.14. Reaction of phenyliodide with methylacrylate under Heck coupling conditions

The experimental procedure reported by Boyes and co-workers [10] was followed.

4. X-ray crystallography

*4.1. Structural analysis of **11***

Crystals for the X-ray structure analysis were grown from a saturated CH_2Cl_2 solution of **11** at r.t. A red prism of $0.50 \times 0.41 \times 0.32$ mm^3 was selected for X-ray analysis. A total of 25 reflections was used for an accurate orthorhombic cell determination. Three reflections and their equivalents were selected to check the Laue group. A total of 4285 reflections were collected at r.t. up to $\sin(\theta)/\lambda = 0.623$ Å^{-1} on an Enraf–Nonius CAD-4 diffractometer. The data were corrected for Lorentz and polarization effects [12] and for absorption (psi-scan method) [13]. No decay was observed. The structure was solved via a Patterson search program [14] and refined in the polar space group $P2_12_12_1$ with full-matrix least squares methods [14] based on $|F^2|$. All non-hydrogen atoms were refined with anisotropic thermal parameters. Hydrogen atoms were included in their calculated positions and refined with a riding model. At the end of this refinement the agreement indices were $wR_2 = 0.0826$ for all data and $R_1 = 0.0297$ for 3807 intensities with $I > 2\sigma(I)$, the absolute structure parameter [15] was $x = 0.06(3)$. The final difference electron density is: $\Delta\rho = 0.618$ and -0.422 e Å^{-3}. Crystal data are reported in Table 5.

*4.2. Structural analysis of **12***

Crystals for the X-ray structure analysis were grown from a saturated CH_2Cl_2 solution of **12** at r.t. A brown–red block of $0.20 \times 0.18 \times 0.12$ mm [14] was selected for X-ray. A total of 15 555 reflections were collected at 153 K on a Siemens SMART CCD diffractometer. An empirical (SHELXTL-PLUS) absorption correction was applied. The structure was solved by direct methods [14] and refined by full-matrix least squares methods [14] based on 8977 unique $|F^2|$. All non-hydrogen atoms were refined with anisotropic thermal parameters. Hydrogen atoms were found from difference Fourier synthesis and refined with isotropic thermal parameters. At the end of this refinement the agreement indices were $wR_2 = 0.0957$ for all data and $R_1 = 0.0342$ for 8036 intensities with $I > 2\sigma(I)$. The final difference electron density is: $\Delta\rho = 0.636$ and $-$ 0.608 e Å^{-3}. Crystal data are reported in Table 5.

5. Supplementary material

Crystallographic data (excluding structural factors) for the structures has been deposited with the Cambridge Crystallographic Data Center, CCDC no. 142833 for compound **11** and CCDC no. 142834 for compound **12**. Copies of the data can be obtained free of charge from The Director, CCDC, 12 Union Road, Cambridge CB2 1EZ, UK (Fax: +44-1223-336033; e-mail: deposit@ccdc.cam.ac.uk or www: http://www.ccdc.cam.ac.uk).

Acknowledgements

We thank S. Gourier for technical assistance. L.G. Kuz'mina acknowledges Judith A.K. Howard, University of Durham, UK, for the structure solving of **12** in her laboratory.

References

[1] R. Broussier, M. Laly, P. Perron, B. Gautheron, I.E. Nifant'ev, J.A.K. Howard, L.G. Kuz'mina, Ph. Kalck, J. Organomet. Chem. 587 (1999) 104.

[2] U. Castellato, B. Corain, R. Graziani, B. Longato, G. Pilloni, Inorg. Chem. 29 (1990) 1193.

[3] R. Choukroun, D. Gervais, J. Jaud, Ph. Kalck, F. Senocq, Organometallics 5 (1986) 67.

[4] Ph. Kalck, C. Randrianalimana, M. Ridmy, A. Thorez, H.T. Dieck, J. Ehlers, New J. Chem. 12 (1988) 679.

[5] J. Wachter, F. Jeanneaux, G. Le Borgne, J.G. Riess, Organometallics 3 (1984) 1034.

[6] T. Hayashi, M. Konishi, Y. Kobori, M. Kumada, T. Higuchi, K. Hirotsu, J. Am. Chem. Soc. 106 (1984) 158.

[7] I.A. Butler, W.R. Cullen, T.J. Kim, S.J. Rettig, J. Trotter, Organometallics 4 (1985) 972.

[8] T. Hayashi, M. Kumada, T. Higuchi, K. Hirotsu, J. Organomet. Chem. 334 (1987) 195.

[9] T. Chenal, R. Naigre, I. Cipres, Ph. Kalck, J.C. Daran, J. Vaissermann, J. Chem. Soc. Chem. Commun. (1993) 747.

[10] A.L. Boyes, I.R. Butler, S.C. Quayle, Tetrahedron Lett. 39 (1998) 7763.

[11] R. Broussier, E. Bentabet, P. Mellet, O. Blacque, P. Boyer, M.M. Kubicki, B. Gautheron, J. Organomet. Chem. 598 (2000) 365.

[12] K. Harms, University of Marburg, 1996.

[13] (a) A.C.T. North, D.C. Phillips, F.S. Mathews, Acta Crystallogr. Sect. A 24 (1968) 351. (b) A.L. Spek, Acta Crystallogr. Sect. A 46 (1990) C34.

[14] G.M. Sheldrick, SHELXS-97 and SHELXL-97, University of Göttingen, Germany, 1997.

[15] H.D. Flack, Acta Crystallogr. Sect. A 39 (1983) 876.

[16] (a) M.N. Burnett, C.K. Johnson, ORTEP-III, Oak Ridge Thermal Ellipsoid Plot Program for Crystal Structure Illustrations, Oak Ridge National Laboratory Report ORNL-6895, 1996. (b) L.J. Farrugia, J. Appl. Crystallogr. 30 (1997) 565.